

Supplementary Figure Legends

Supplementary Figure S1: The promoters of the Pumilio complex are bound and regulated by the dREAM complex in *Drosophila*

(A) Relative RT-PCR levels from IgG, RBF1, E2F1 and E2F2 ChIP from *Drosophila* larvae of the *actin*, *brat*, *pumilio* (*pum*) and *nanos* (*nos*) gene transcription start sites (TSS) and genomic region (gene). (B) Relative probe intensities from ChIP-chip assays of dREAM (E2F2, Myb, Mip120, Mip130 and Lin-52) components on the promoter of the Pum complex members (Georlette et al, 2007). (C) Relative RT-PCR levels of *e2f1*, *dp1*, *e2f2* and *rbf1* from adult females expressing Arm-Gal4, UAS-RNAi constructs. (D) RT-PCR of *e2f2*, *pumilio*, *nanos* (*nos*) and *brat* from E2F2 heterozygote mutants (*e2f2/T2Δ3*) and E2F2 homozygote mutant (*e2f2/e2f2*) females.

Supplementary Figure S2: dREAM components regulate Pumilio complex expression

(A) Relative RT-PCR levels of tubulin (*tub*), *pumilio* (*pum*), *brat* and *nanos* (*nos*) from *Drosophila* S2 cells transfected with dsRNA targeting Luciferase (*Luc*), E2F1 and E2F2. (B) Relative expression levels of *tub*, *e2f1* and *e2f2* following dsRNA treatment of S2 cells. (C) Relative expression of *pum*, *nos* and *brat* from Kc cells following depletion of dREAM components, Mip120, Mip130, Myb, E2F2, Rbf1/2, Lin32, Mip40 and *l(3)mbt* (Georlette et al, 2007). (D) Relative Luciferase levels from reporter constructs containing the *pumilio*, *nanos* and *brat* promoters upstream of the Luciferase gene from S2 cells depleted of GFP, E2F1, E2F2 or RBF1.

Supplementary Figure S3: The human pocket proteins regulate the expression of the mammalian PUM complex

(A) RT-PCR results for PUM components (PUM1, PUM2, NANOS1, NANOS2 and NANOS3), E2F target (*Cyc A*) and non-E2F target (*E2F3*) from BJ fibroblast cells transfected with siRNA pools targeting the pocket proteins (*Rb1*, *p107* and *p130*) individually and in combination. (B) Western blots of NANOS1 (NOS1), PUMILIO1 (PUM1), PUM2, *Rb1*, *p107*, *p130* and Tubulin (TUB) from BJ cells transfected with siRNAs targeting the pocket proteins. (C) Western blots of NOS1, PUM1, PUM2, *Rb1*, *p107*, *p130* and Tubulin (TUB) from RPE cells transfected with siRNAs targeting the pocket proteins.

Supplementary Figure S4: Rb1 loss diminishes pocket protein binding to the NANOS1 promoter

(A) Relative RT-PCR levels of *CDC6* (E2F target gene), the NANOS1 promoter (NOS1 Prom) and -1000bp upstream of the NANOS1 TSS in IgG (-ve control), E2F4, *p130* and *p107* ChIP's from BJ cells depleted for scrambled control sequences (Scr) or RB using siRNA. (B) Relative RT-PCR levels of *CDC6*, the NANOS1 transcription start site (TSS), -1000bp upstream of the NANOS1 TSS and the NANOS1 3'UTR in IgG (-ve control), E2F4, *p130* and *p107* ChIP's from Y79 Retinoblastoma cells.

Supplementary Figure S5: p16 and CDK inhibitors effect NANOS expression

(A) Relative RT-PCR results of p16, NANOS1-3 and PUM1-2 from BJ cells depleted of p16 using shRNA. **(B)** Drug sensitivity assay of HCT116 cells treated with the CDK4/6 inhibitor PD0332991 (PD) or DMSO for 4 days. **(C)** Relative RT-PCR results of NANOS1-3 and PUM1-2 from HCT116 cells treated with DMSO or PD0332991 (PD) at 1 μ M or 100nM concentrations.

Supplementary Figure S6: NANOS1 expression is antiF correlated with Rb1 levels

(A) Correlation and p-value of PUM1, PUM2, NANOS1, NANOS2 and NANOS3 expression with Rb1 levels from a broad panel of cancer cell lines (Barretina et al, 2012). **(B)** Correlation and p-value of PUM1, PUM2, NANOS1, NANOS2 and NANOS3 with Rb1, Rbl1 (p107) and Rbl2 (p130) expression from cancer cell line expression database. **(C)** Correlation and p-value of PUM1, PUM2, NANOS1, NANOS2 and NANOS3 with the Rb1 loss signature (Herschkowitz et al, 2008). **(D)** NANOS1 expression levels in NSCLC cells in cells retaining Rb1 and p53 activity, compared to cells lacking p53 and Rb1 respectively. **(E)** NSCLC cell lines used for analysis in Supp Fig 4D. **(F)** Relative NANOS1 expression levels from the Sanger cancer cell line encyclopedia in cancer cells expressing low, average and high levels of Rb1.

Supplementary Figure S7: Heat map of the correlation between PUM/ NANOS with the Rb1 loss signature

(A) Heat map of the correlation between PUM1, PUM2, NANOS1, NANOS2 and NANOS3 and each gene in the Rb1 loss signature (Herschkowitz et al, 2008).

Supplementary Figure S8: Genetic interaction between Pum components and RBF1 and E2F2

(A) Images of wing phenotypes from crosses of Nub-Gal4 or Nub-Gal4; Rbf1-RNAi females were mated with males carrying UAS-RNAi constructs targeting the PUM complex (PUM, Nos and Brat RNAi) or mutants with deficiencies in the brat locus (*Brat^{ts1}* and *Brat¹*). **(B)** Images of wing phenotypes from En-Gal4; E2F2 RNAi females crossed to UAS-RNAi constructs targeting Gal4, Pum, Nos and Brat. **(C)** Images of wings from UAS-Dicer; Nub-Gal4 and UAS-Dicer; Nub-Gal4; Gal4 RNAi crosses to individual RNAi constructs targeting, Pum, Nos, Brat, Luc and Gal4.

Supplementary Figure S9: Rb1 and Nanos1 depletion reduces murine cell number

(A) Relative RT-PCR of Rb1, p107 and p130 from wild-type (wt), Rb1 mutant (Rb1-/-), p107 mutant (p107-/-), p130 mutant (p130-/-) and Rb1, p107 and p130 mutant (triple) 3T3s. **(B)** Western blots of Nanos1, Pum2 and TUB from wild type 3T3 cells depleted with shRNAs targeting Nanos1 (N1-3 and N1-4), Pum2 (P2-1 and P2-5) and scrambled controls (Scr). **(C)** Crystal violet staining of wild-type (duplicate of Figure 3A) and triple-mutant 3T3s (Rb, p107 and p130 -/-) with shRNAs targeting Nanos1 (mNos1-3 and mNos1-4) or a scrambled control sequence (Scr). **(D)** Relative RT-PCR of Nanos1, Pum1 and Pum2 mouse 3T3 cells infected with shRNAs targeting Nanos1, Pum1, Pum2 and Scrambled

(Scr) sequences. **(E)** Quantification of wild-type, Rb1 null (Rb -/-), p107 null (p107-/-), p130 null (p130-/-) and triple negative (Rb1, p107 and p130 -/-, triple -/-) mouse 3T3 cells infected with shRNA targeting Nanos1, Pum1 and Pum2.

Supplementary Figure S10: Depletion of NANOS1 and pRb reduces human cell number

(A) Relative RT-PCR levels of Nanos1-3, Pum1-2, Cyclin A (Cyc A) (E2F target gene) and E2F3 (non-E2F target) in wild type, *Rb1* -/-, *p107* -/-, *p130* -/- and triple-mutant (*Rb1*, *p107* and *p130* -/-) 3T3 cells. **(B)** Relative RT-PCR levels of p16 in wild type (wt), *Rb1* null (Rb-/-), *p107* null (p107-/-) and *p130* null (p130-/-) 3T3 cells. **(C)** Western blots of Tubulin (TUB), pRb and NANOS1 (NOS1) from BJ cells infected with shRNAs targeting pRb (E3, D4 and D5), NANOS1 (N1-1 and N1-3) and scrambled (Scr sequences). **(D)** Crystal violet staining of Calu-1 cells infected with shRNAs targeting Rb1 (Rb1 E3 and Rb1 D4), NANOS1 (hNOS1-1 and hNOS1-3) and scrambled (Scr) sequences.

Supplementary Figure S11: Functional p53 is necessary for Rb1 and NANOS1 silencing to affect cell number in cancer cell lines

(A) Quantification of cell staining in cancer cell lines after depletion of NANOS1 (NOS1-3 and NOS1-4) and control scrambled sequences (Scr). P-value: *p<0.05, **p<0.01. **(B)** Extended table and crystal violet staining of cancer cell lines tested for synthetic lethality phenotype. The table details each cell lines Rb1/p16 and TP53 status and whether a synthetic lethality phenotype was observed upon NANOS1 depletion. Cell lines are boxed according to tissue: white =non-transformed controls, yellow box =NSCLC cells, blue=bladder, pink=breast, orange=head and neck, red=293T, grey=colorectal, olive=bone. **(C)** Quantification of cell staining of isogenic HCT116 cells retaining or lacking p53 activity after depletion of NANOS1 or scrambled control. P-value: *p<0.05.

Supplementary Figure S12: NANOS1 depletion reduces cell number in pRbF deficient cancer cells

(A) Growth curve of Y79 Retinoblastoma cells depleted of NANOS1 or scrambled control (Scr) using siRNA. **(B)** Growth curve of NCI-H1666 cells depleted of NANOS1 or scrambled control (Scr) using siRNA. **(C)** Relative RT-PCR levels of NANOS1 from Y79 and NCI-H1666 cells treated with a pool of siRNAs targeting NANOS1.

Supplementary Figure S13: Loss of PUM activity stabilizes transcripts downF regulated in Retinoblastoma tumors.

(A) Time course of RNA stability for the MAP3K1 transcript in Y79 Retinoblastoma cells treated with Actinomycin D depleted of PUM1, PUM2 or scrambled control sequence. **(B)** Time course of RNA stability for the MAP2K3 transcript in Y79 Retinoblastoma cells treated with Actinomycin D depleted of PUM1, PUM2 or scrambled control sequence. **(C)** Time course of RNA stability for the E2F4 transcript (non-PRE containing mRNA) in Y79 Retinoblastoma cells treated with Actinomycin D depleted of PUM1, PUM2 or scrambled control

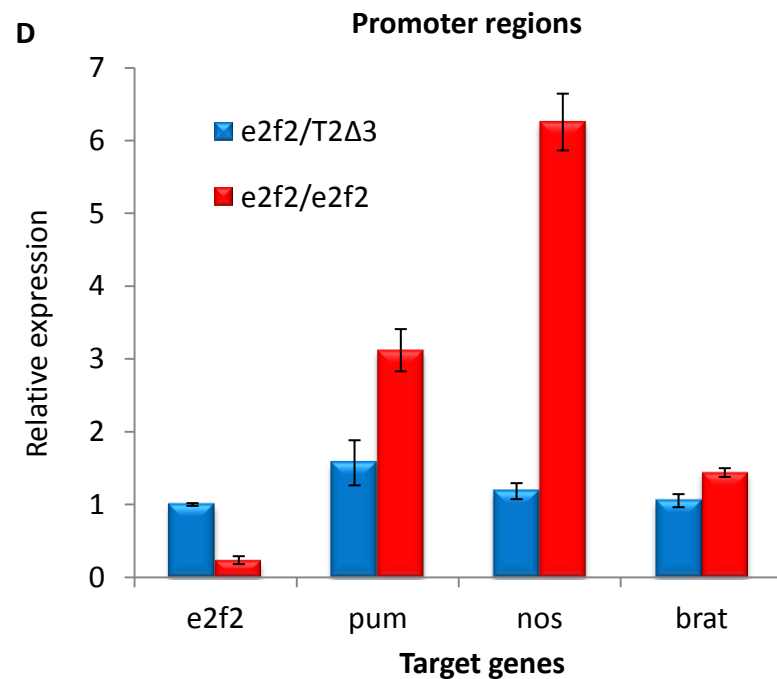
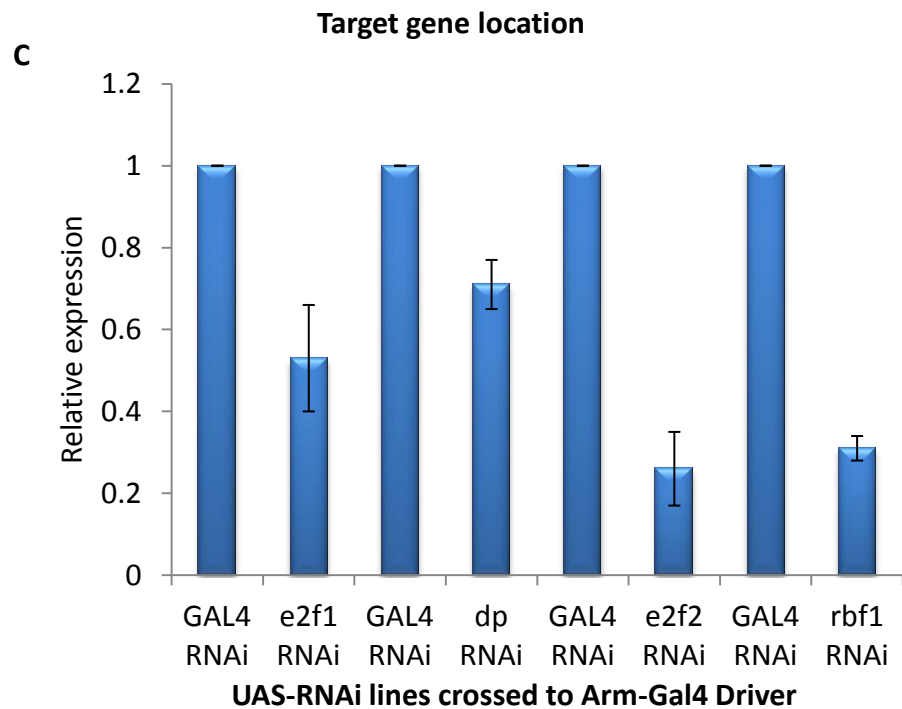
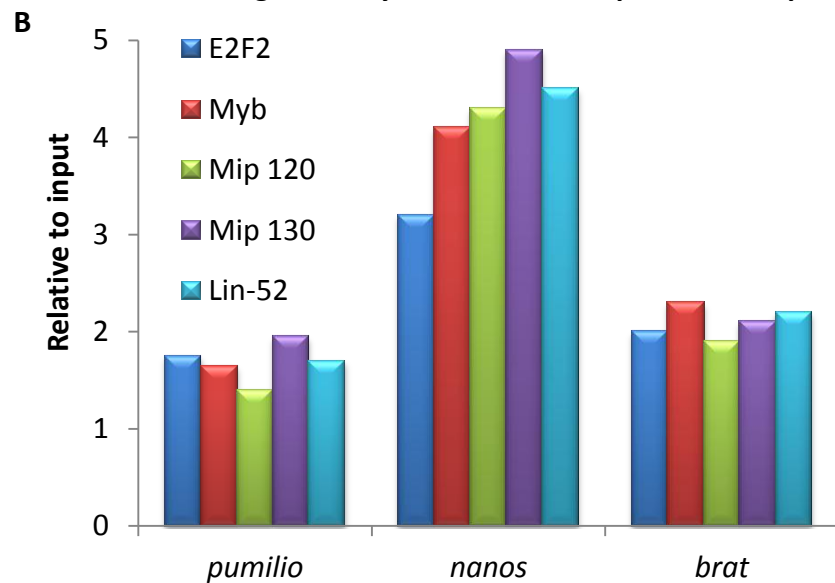
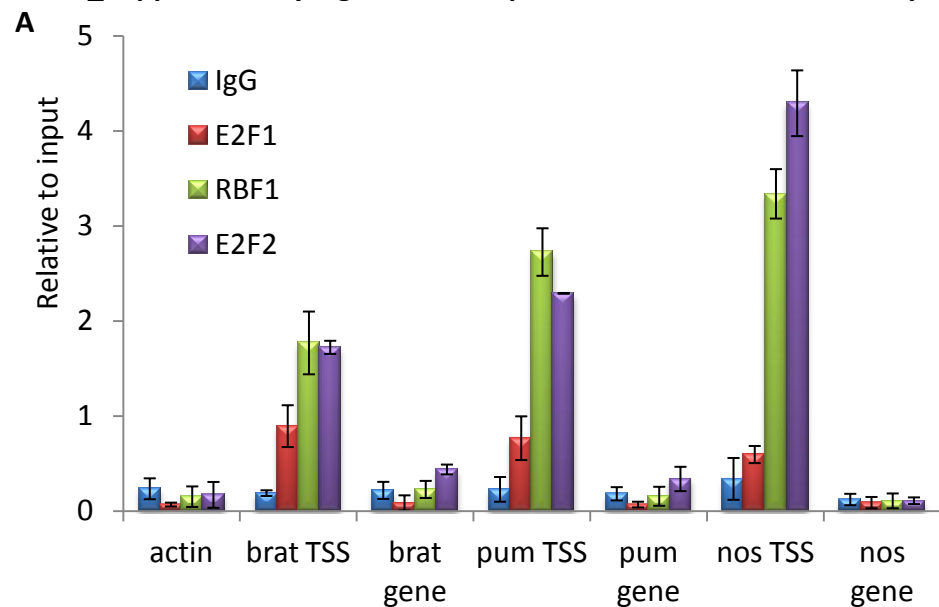
sequence. **(D)** Western blot of Y79 cells treated with shRNAs targeting PUM1 (P1-15 and P1-19) and PUM2 (P2-1 and P2-4).

Supplementary Figure S14: NANOS1 mediated regulation of MAP kinase activity is postF transcriptional.

(A) Western blots from HCT-116 p53^{-/-} cells of PUM1, PUM2, TUB used for Map2K3 Luciferase experiments. **(B)** Western blots of MAP3K1, MAP2K3, NANOS1 and TUB from HCT116 cells depleted with shRNAs targeting NANOS1 (1-1 and 1-3) or scrambled controls (Scr). **(C)** Relative RT-PCR levels of NANOS1, MAP3K1 and MAP2K3 from HCT116 cells depleted with shRNAs targeting NANOS1 (1-1 and 1-3) or scrambled controls (Scr). **(D)** Western blot of MAP3K1 and TUB from HCT116 cells depleted with shRNAs targeting MAP3K1 (1 and 2) and scrambled controls (Scr). **(E)** Quantification of HCT116 cell number upon NANOS1 and MAP3K1 depletion by shRNA.

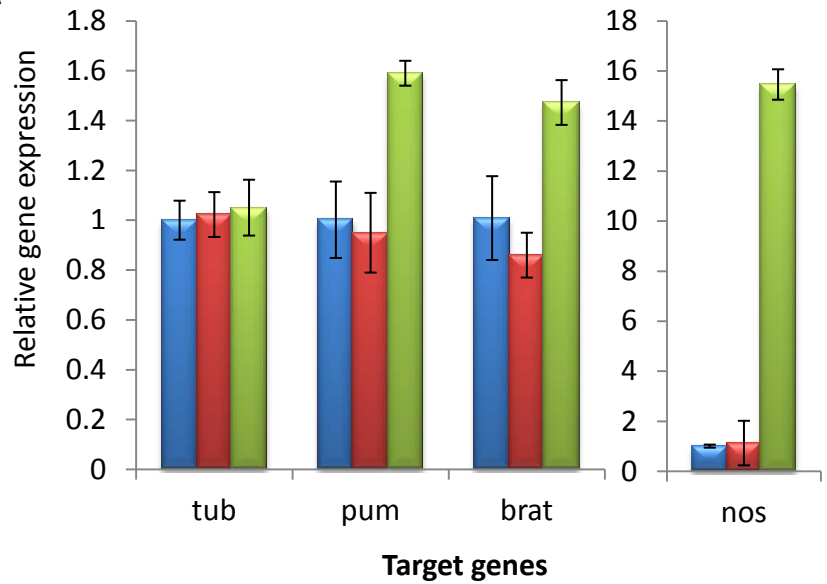
Supplementary Table S1: Genetic interaction between PUM complex members and rbf1 and e2f2

Miles_Supplementary Figure S1: The promoters of the Pumilio complex are bound and regulated by the dREAM complex in *Drosophila*

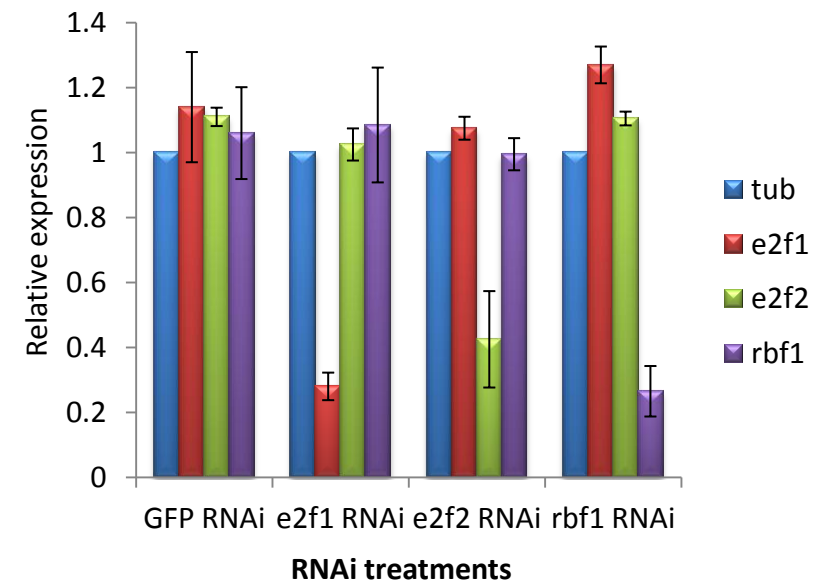


Miles_Supplementary Figure S2: dREAM components regulate Pumilio complex expression

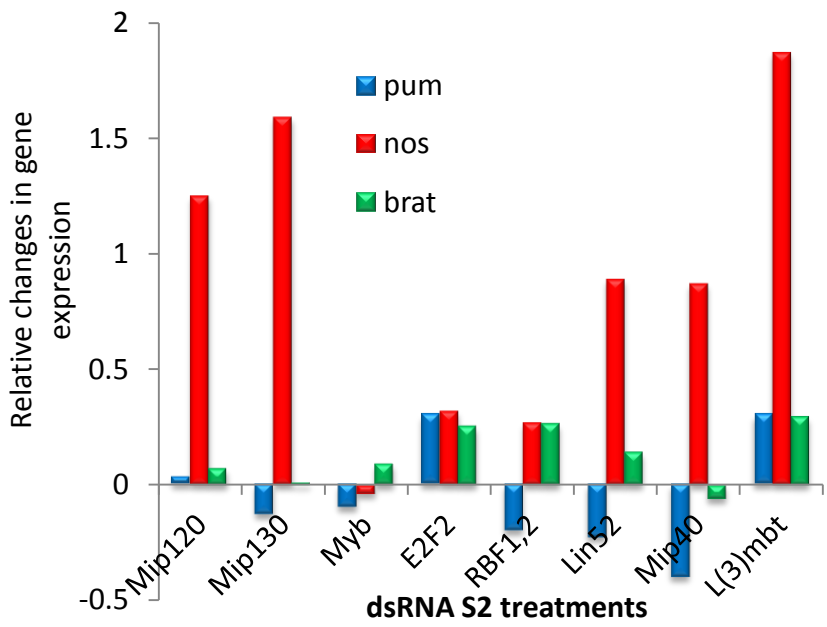
A



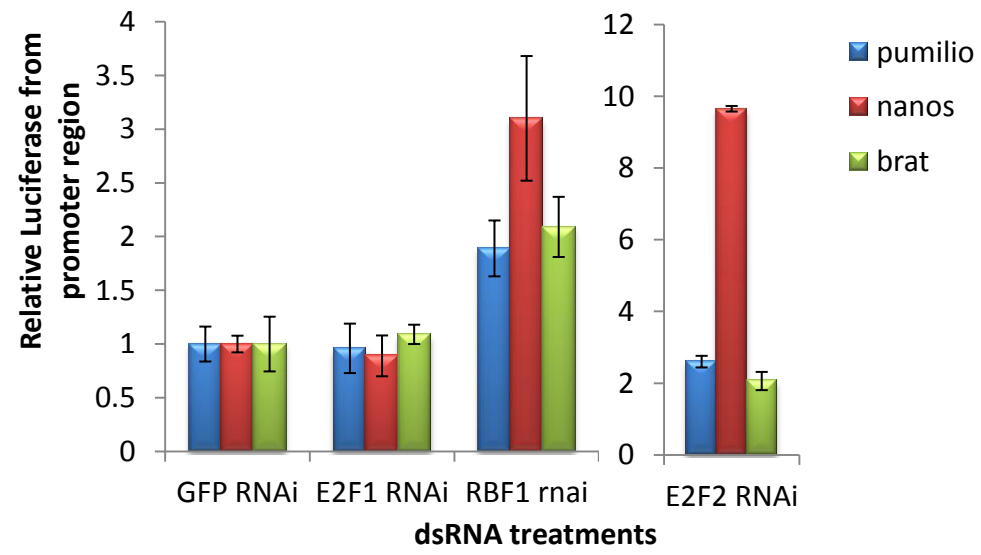
B



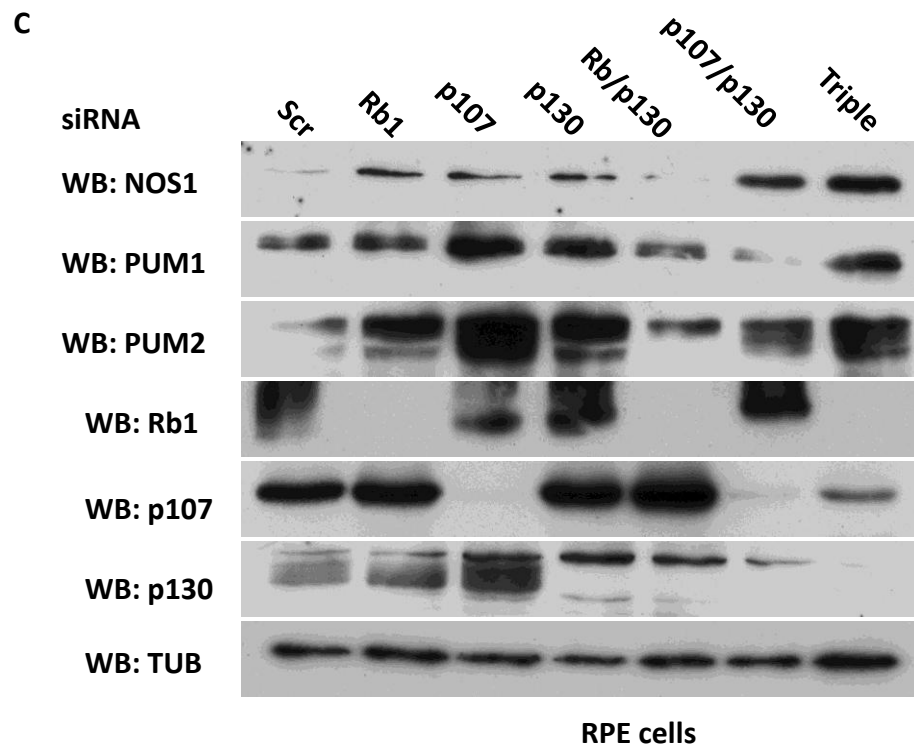
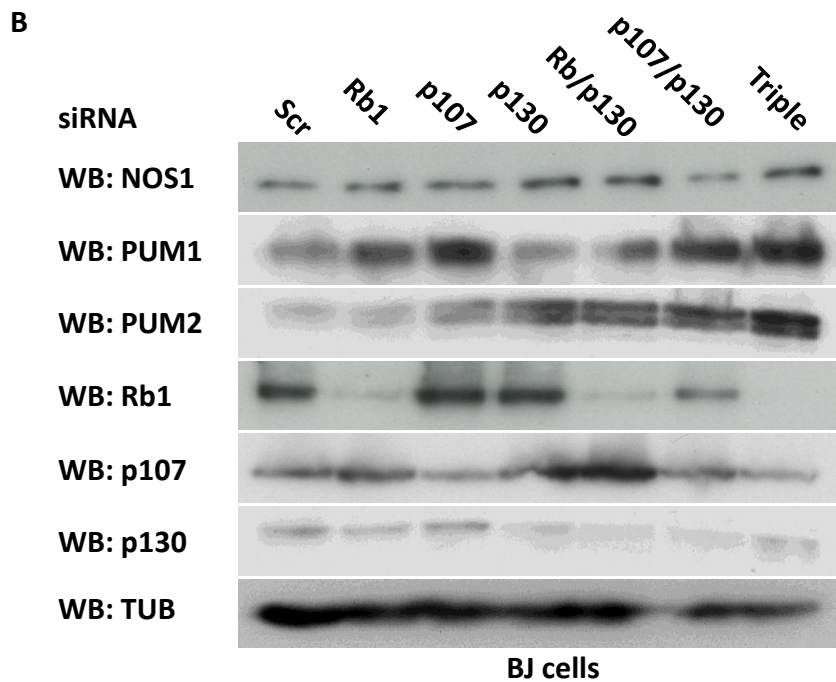
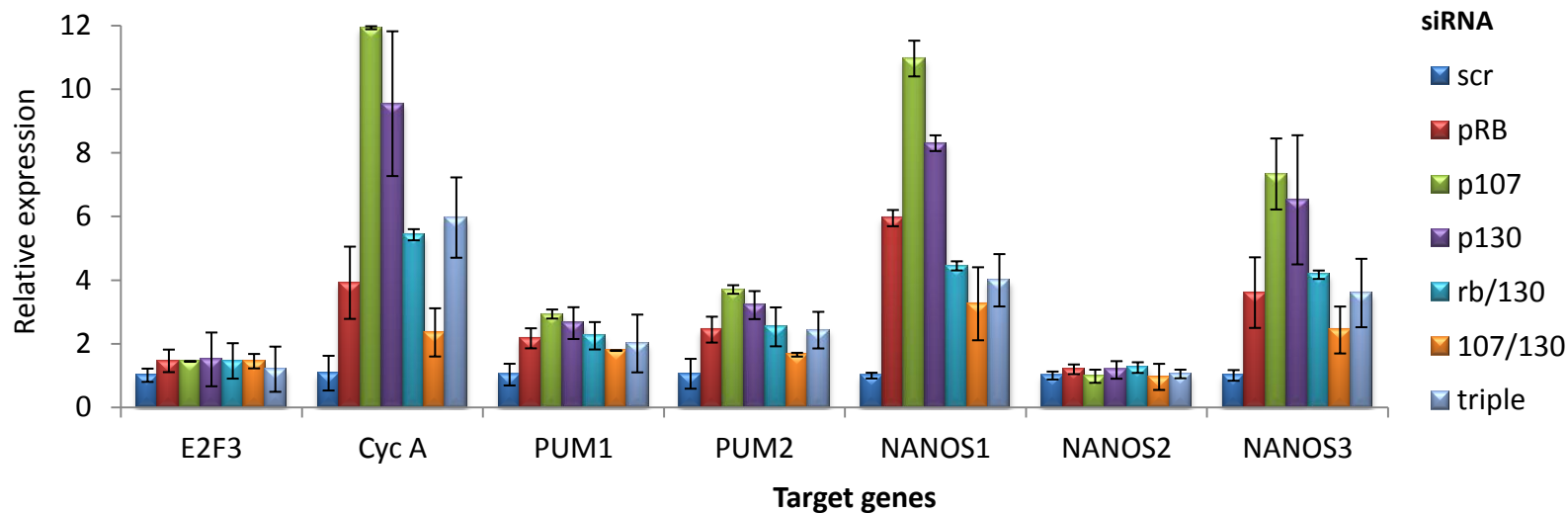
C

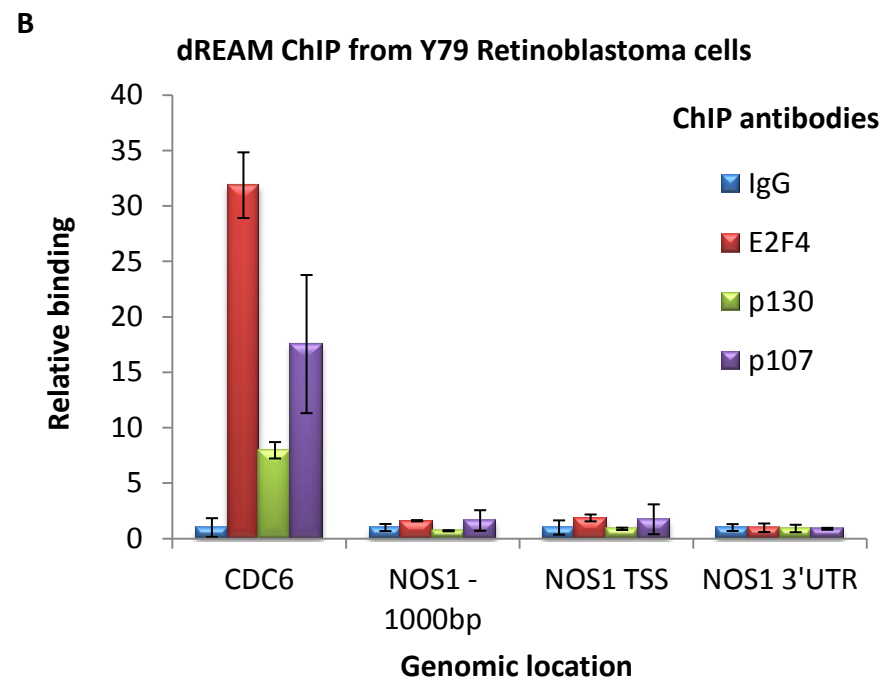
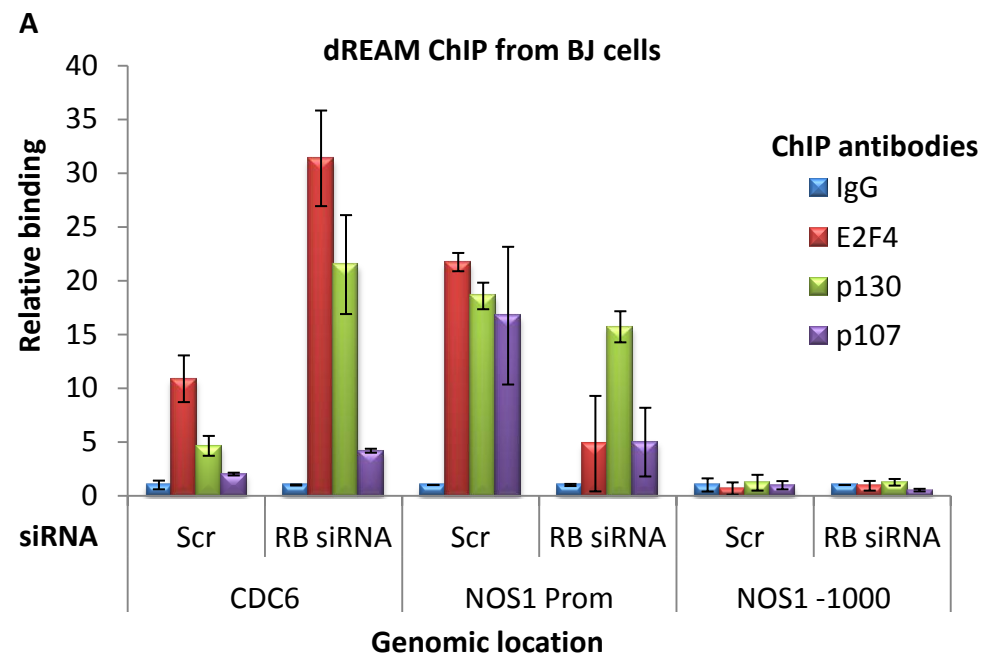


D

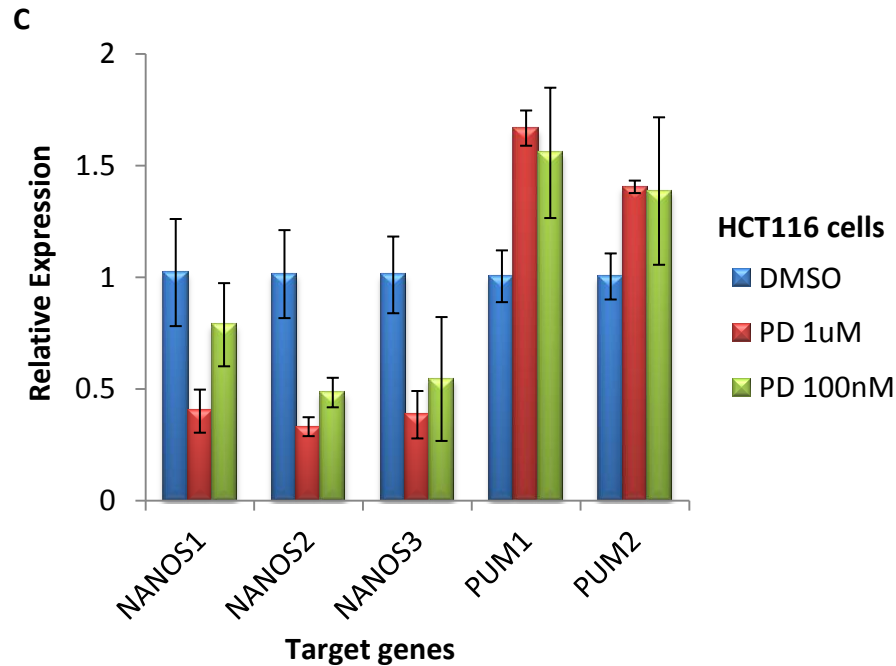
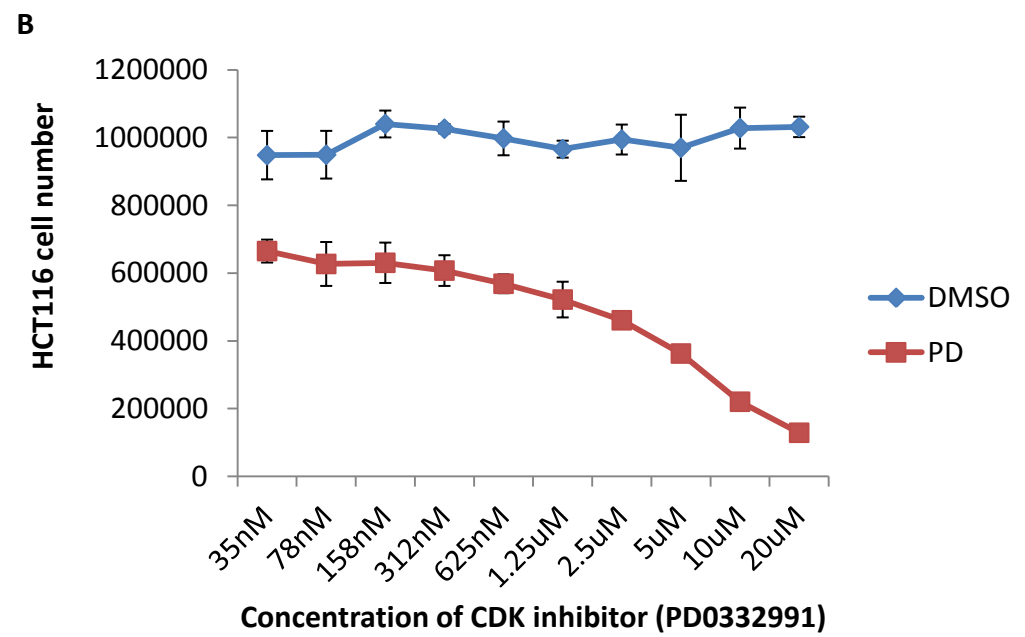
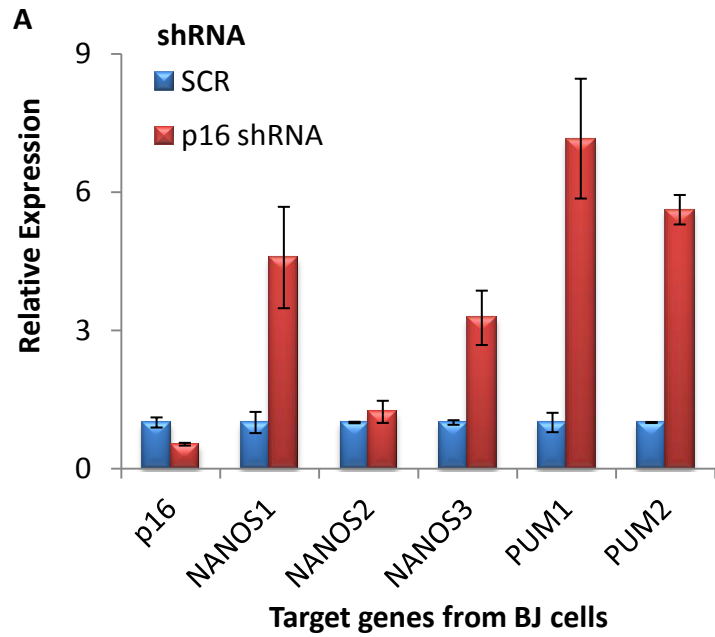


Miles_Supplementary Figure S3: The human pocket proteins regulate the expression of the mammalian PUM complex





Supplementary Figure S4: Rb1 loss diminishes pocket protein binding to the NANOS1 promoter

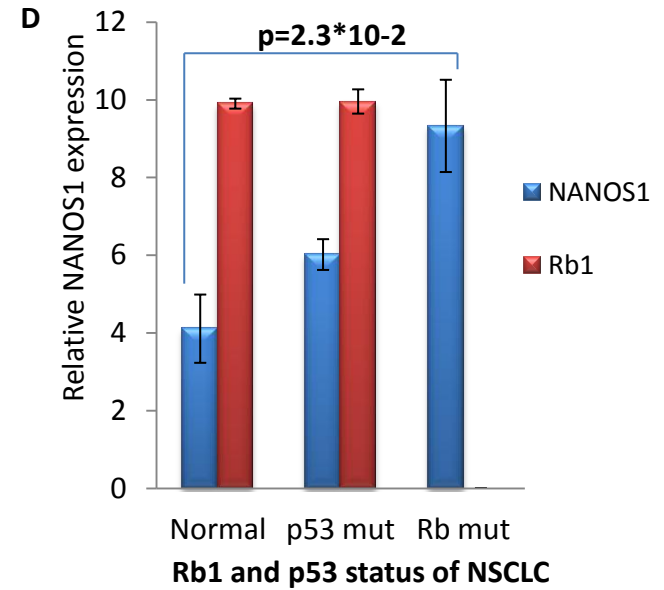


Miles Supplementary Figure S5: p16 and CDK inhibitors effect NANOS

suppression

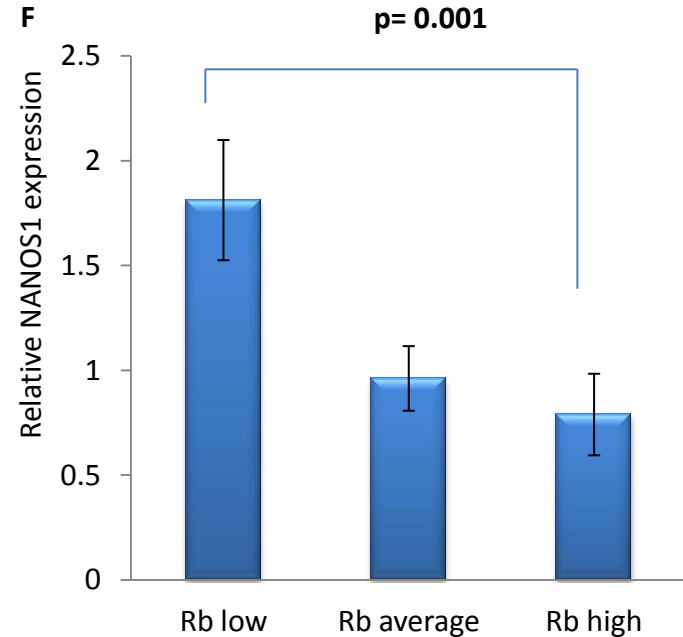
A PUM complex correlation with Rb1 expression

Rb1	tested gene	Correlation with Rb1 expression	p value
Rb1	PUM1	-0.04695035	0.155435
Rb1	PUM2	0.2316398	1.23E-12
Rb1	NANOS1	-0.2422241	1.04E-13
Rb1	NANOS2	0.01336904	0.685987
Rb1	NANOS3	-0.1438667	1.22E-05



B PUM complex correlation with Rb1, Rbl1 and Rbl2 expression

Pum	RB1: corr	RB1: P	RBL1: corr	RBL1: P	RBL2: corr	RBL2: P
NANOS1	-0.242	1.04e-13	-0.114	0.000543	-0.123	0.000182
NANOS2	0.013	0.686	0.127	0.000115	0.042	0.205
NANOS3	-0.144	1.22e-05	-0.092	0.00517	-0.074	0.0248
PUM1	-0.047	0.155	-0.098	0.00302	0.139	2.42e-05
PUM2	0.232	1.23e-12	0.226	4.14e-12	0.242	1.19e-13



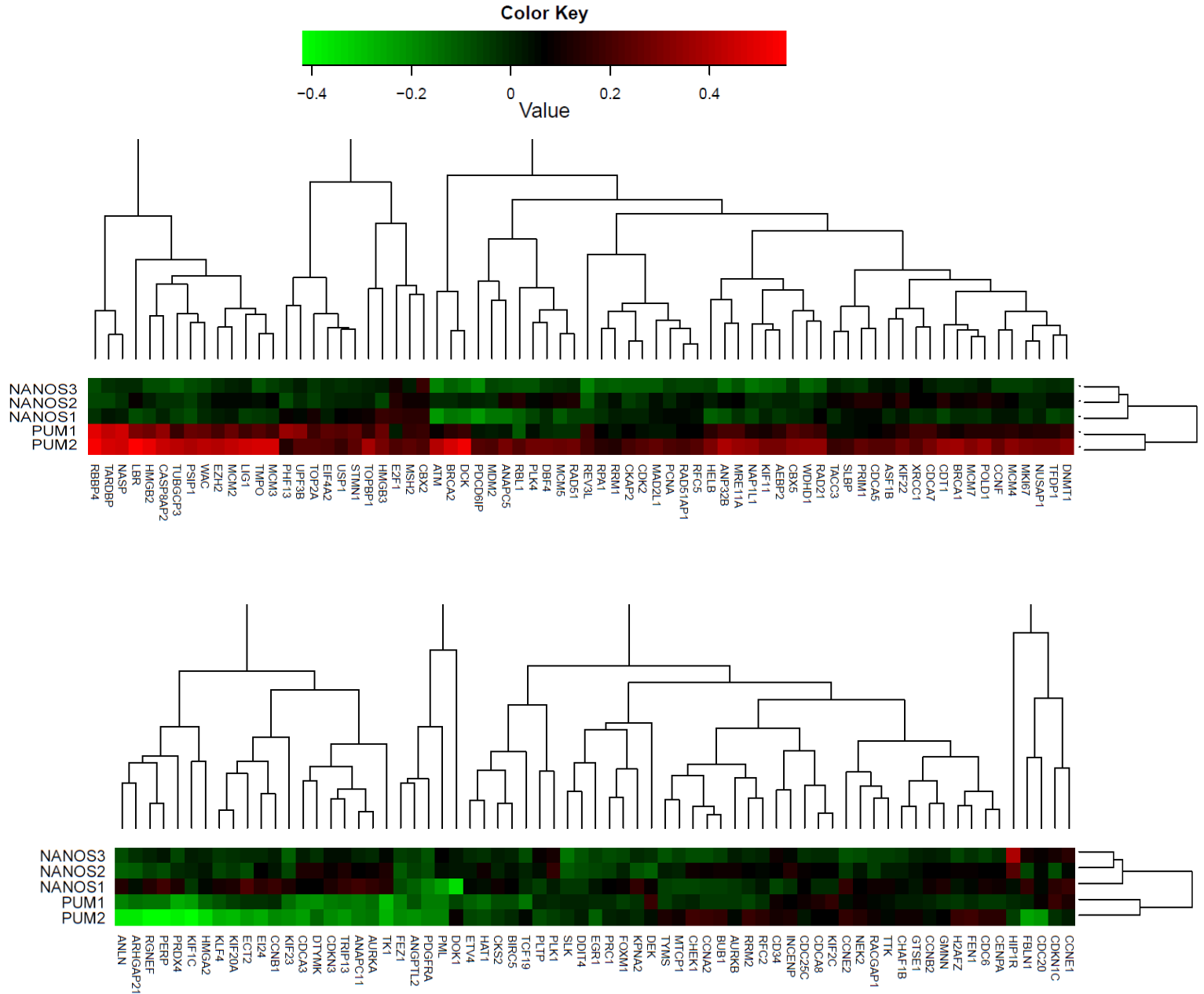
C PUM complex correlation with Rb1 loss signature

tested gene	median corr. signature	median corr. other genes	p value
PUM1	0.039	0.001	5.98E-05
PUM2	0.17	0.029	5.28E-09
NANOS1	0.022	-0.013	0.00026
NANOS2	0.037	0.033	0.394
NANOS3	-0.026	0.013	8.64E-11

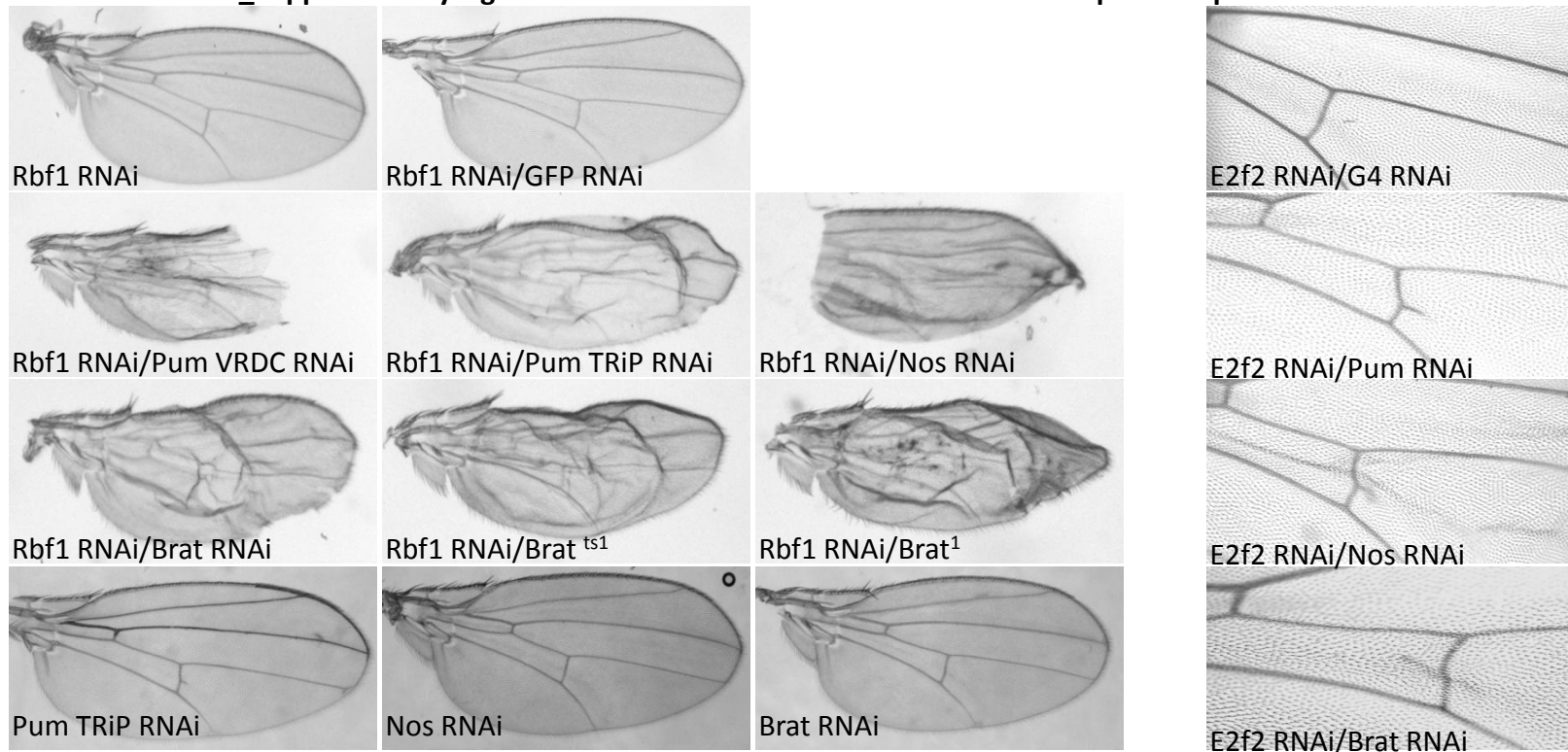
E

	normal	p53 mut	p16/p53 mut
	NCI-H358	NCI-H1573	NCI-H1793
	IMR-90	NCI-H1703	NCI-H596
	COR-L 105		NCI-H1734
	WI 38		NCI-H2228
	Hs 894(E).Lu		NCI-H1563
	Hs 417.Lu		NCI-H1693

Miles_Supplementary Figure S7: Heat map of the correlation between PUM/NANOS with the Rb1 loss signature

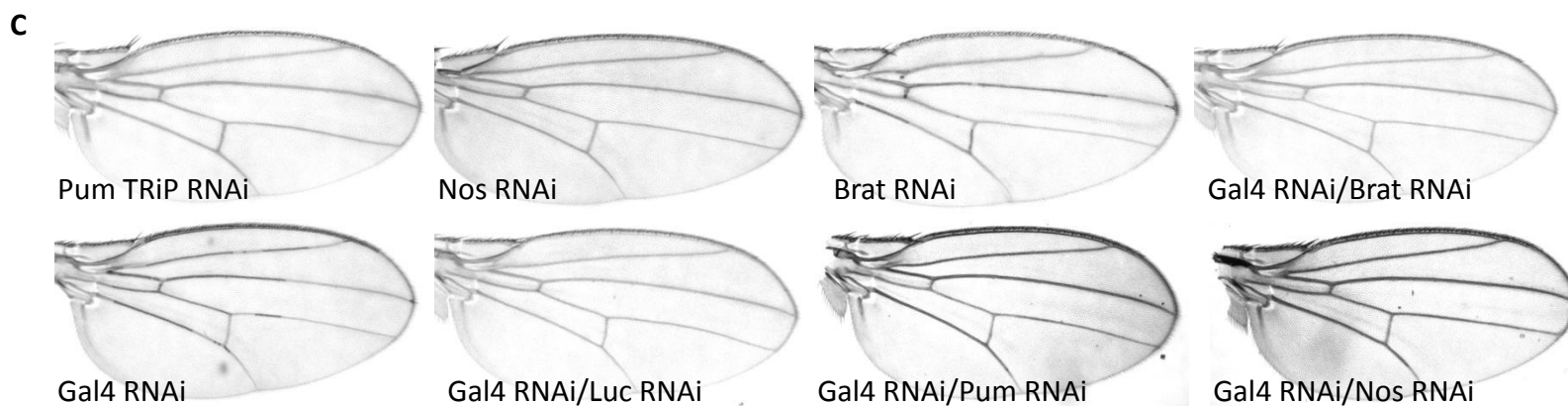


A Miles_Supplementary Figure S8: Genetic interaction between Pum complex components and RBF1 and E2F2



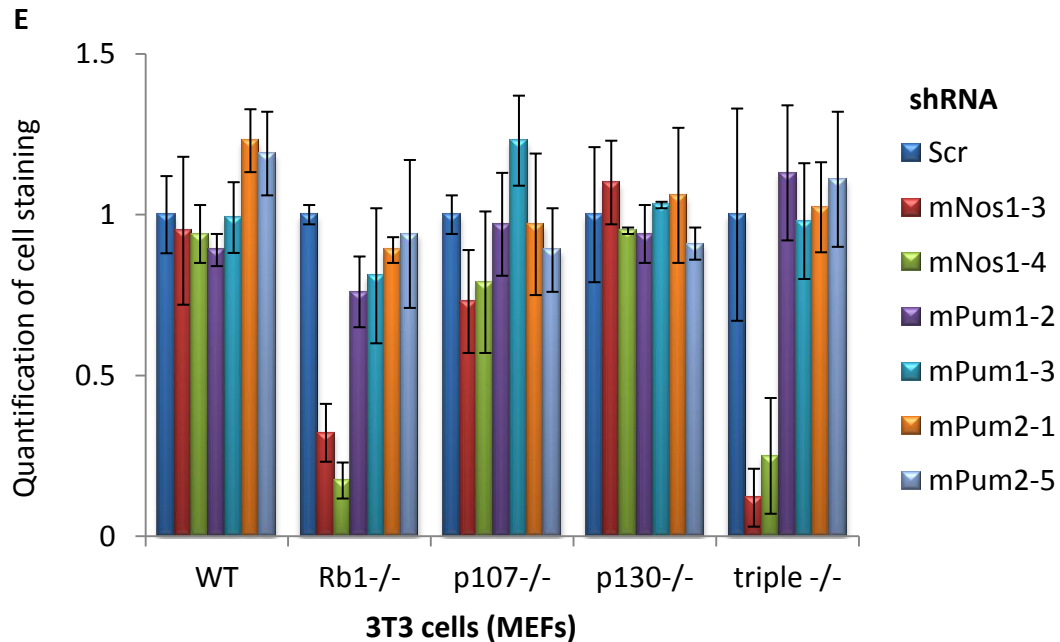
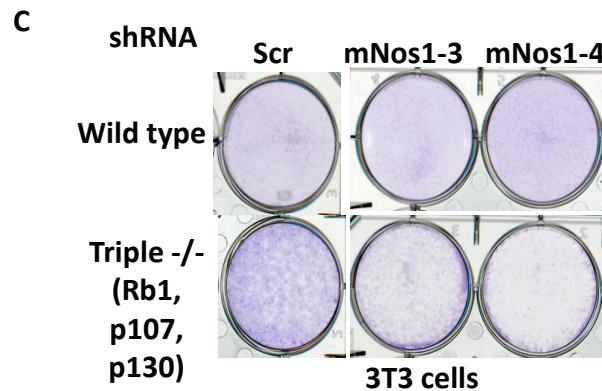
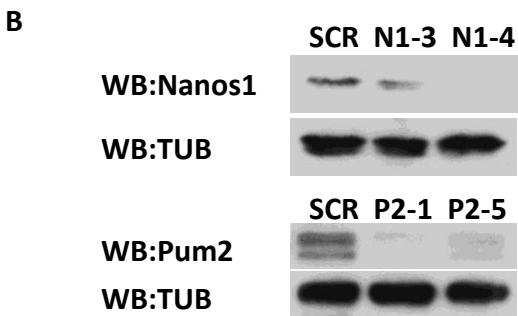
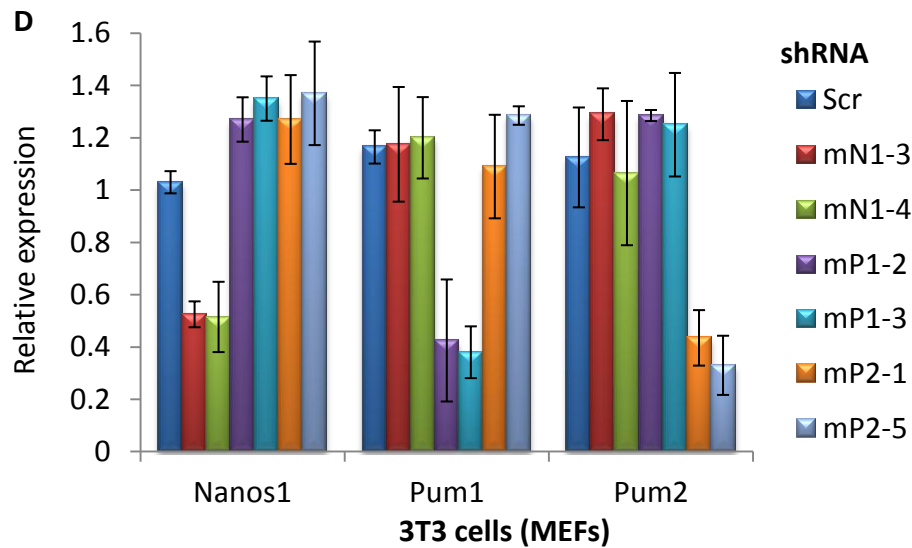
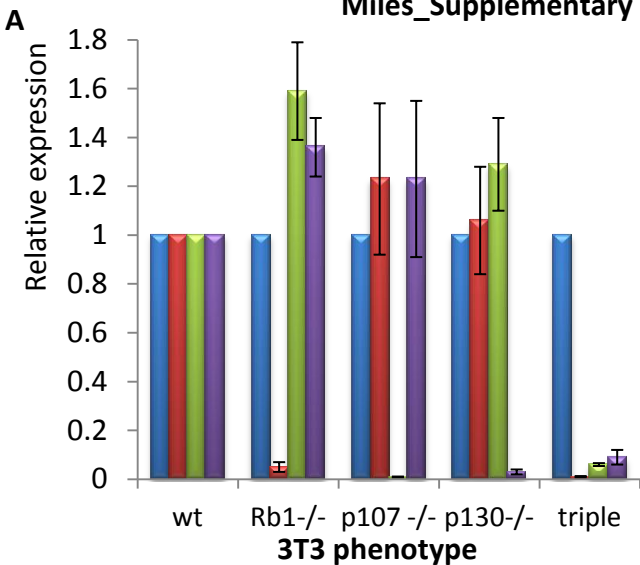
Nub-Gal4 crosses

En-Gal4 crosses



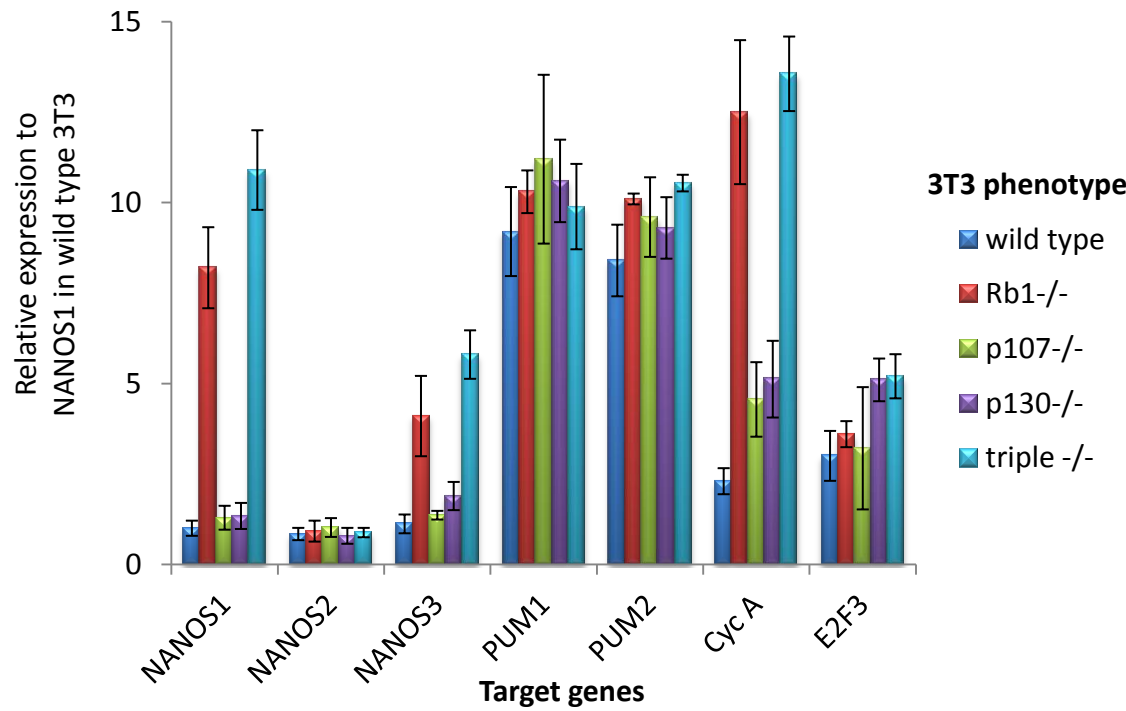
UAS-DICER; Nub-Gal4 crosses

Miles_Supplementary Figure S9: Rb1 and Nanos1 depletion reduces murine cell number

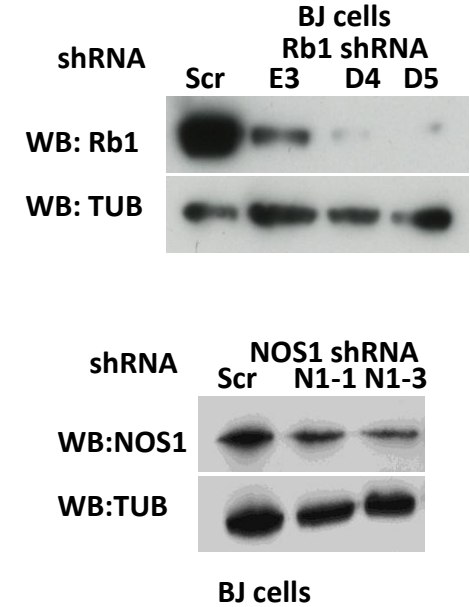


Miles Supplementary Figure S10: Depletion of NANOS1 and pRb reduces human cell number

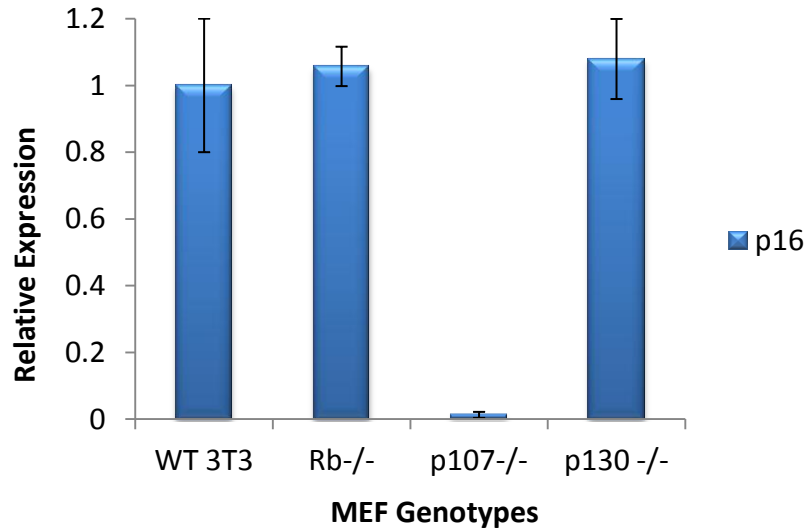
A



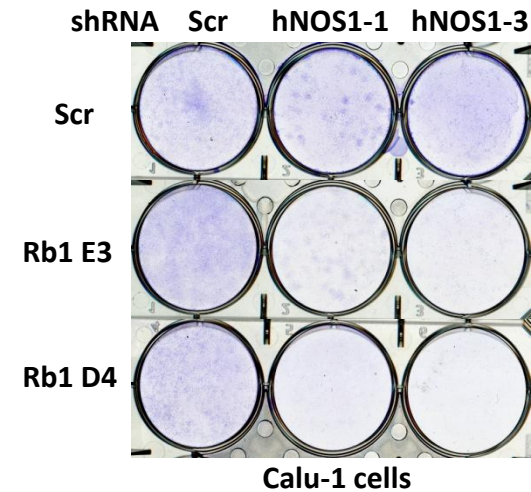
C



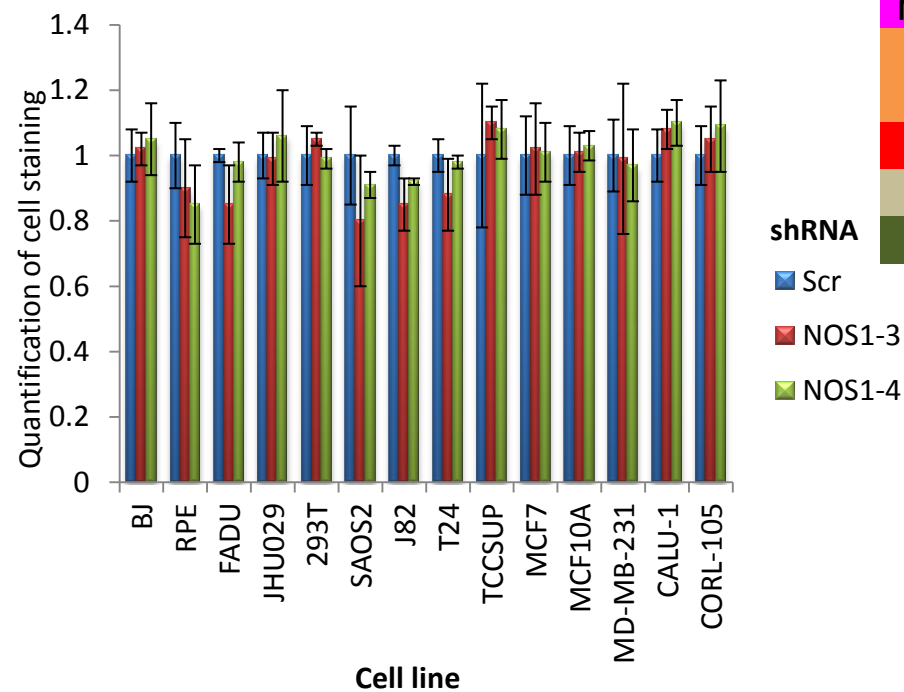
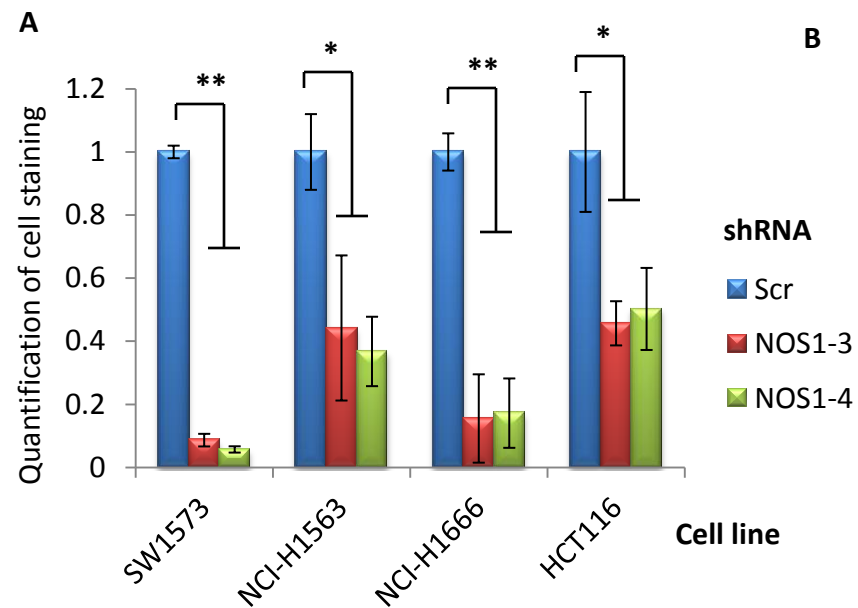
B



D

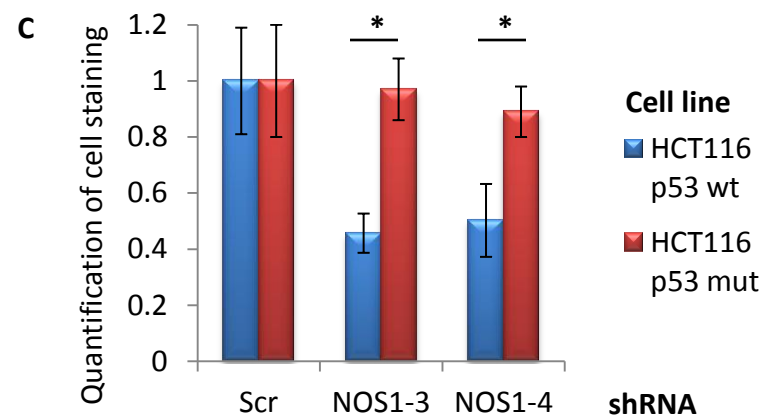


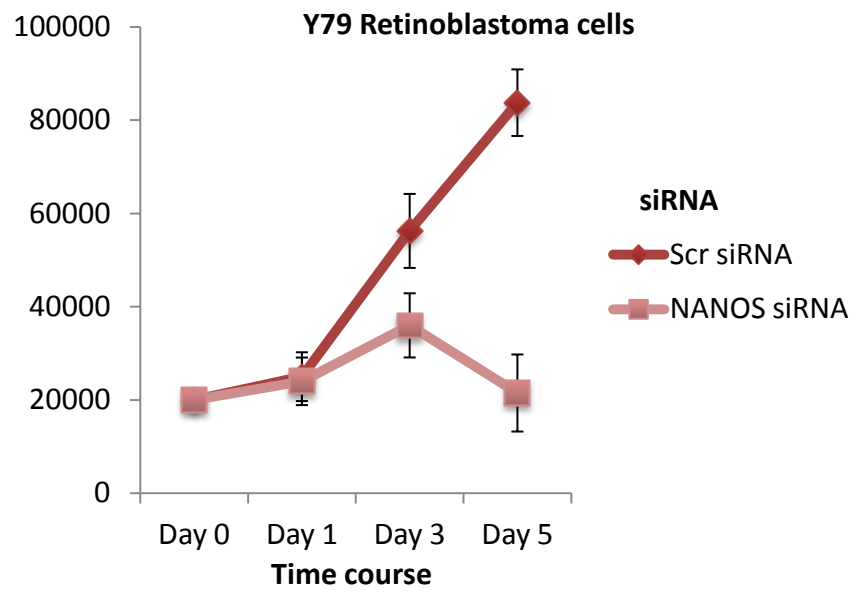
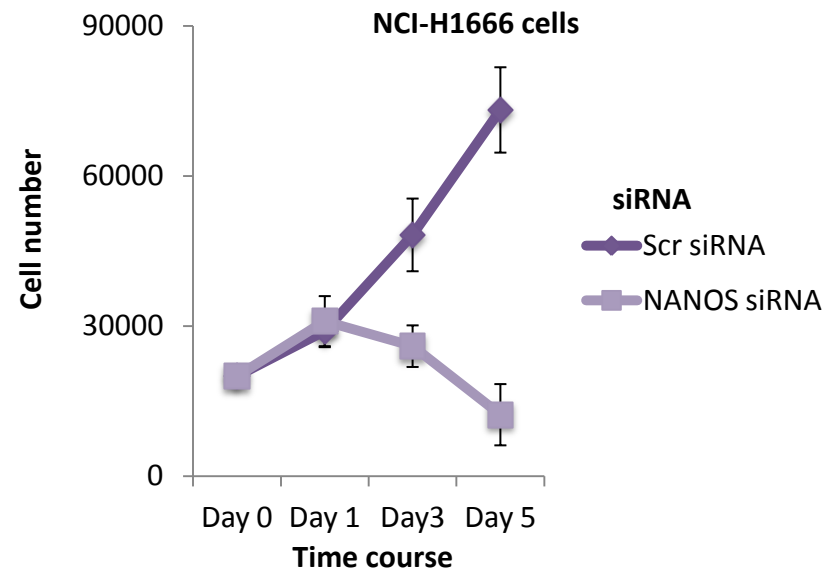
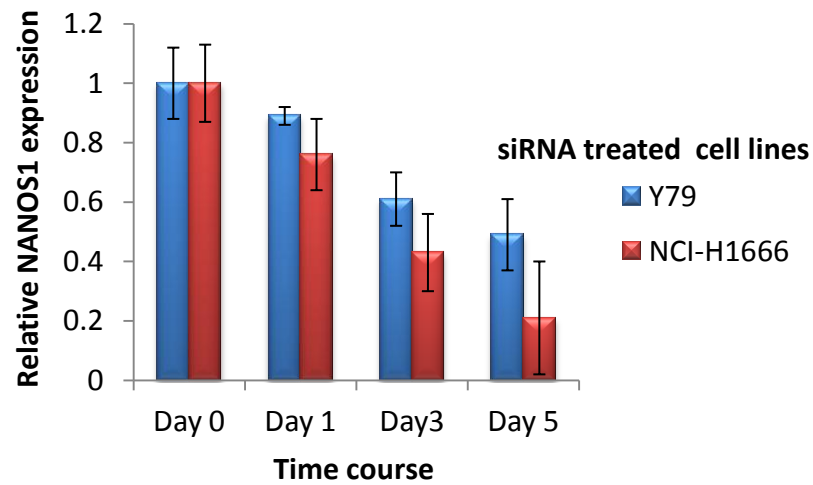
Miles_Supplementary Figure S11: Functional p53 is necessary for Rb1 and NANOS1 silencing to affect cancer cell number



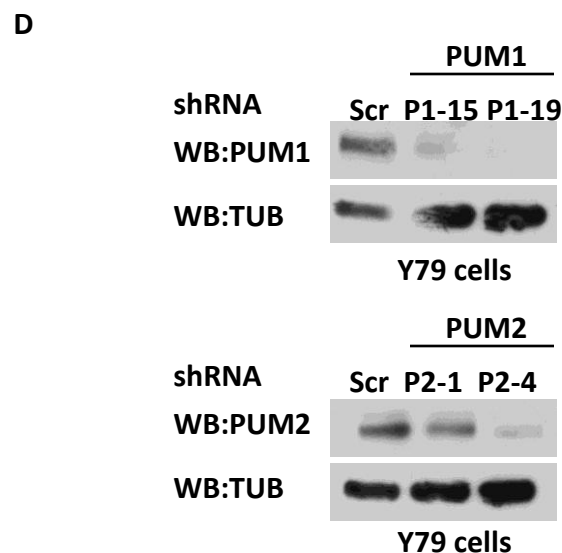
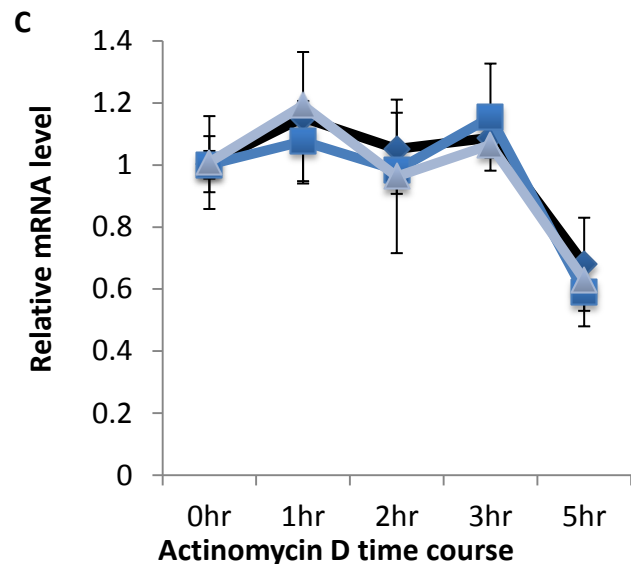
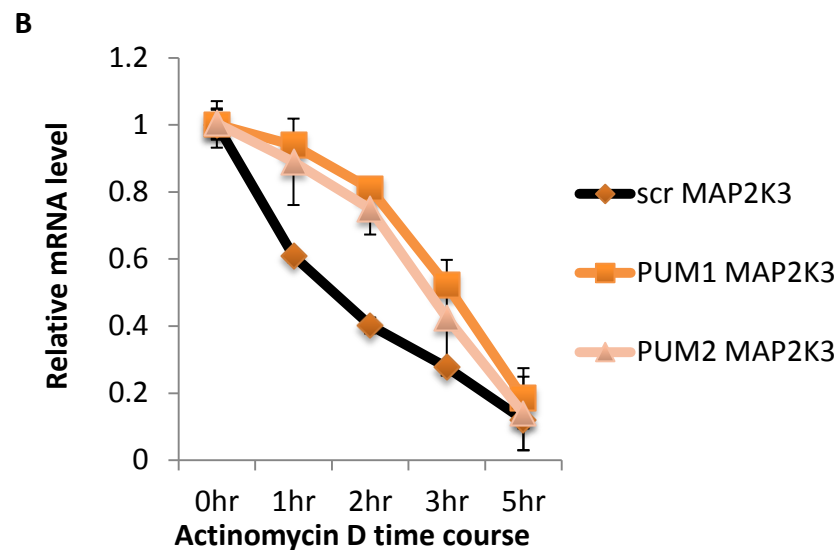
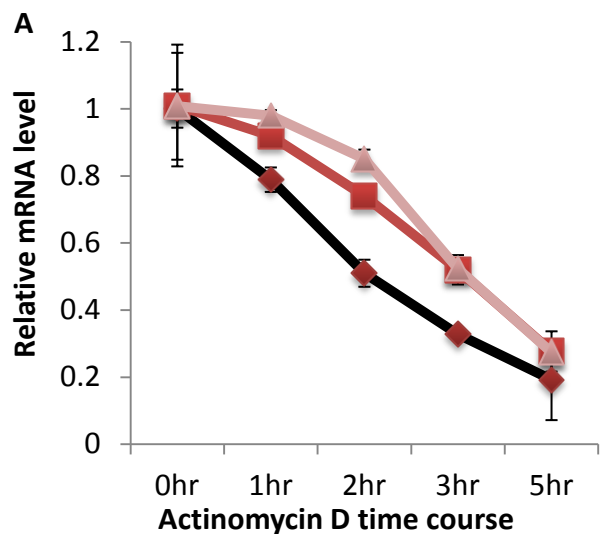
B

Cell lines	Rb1/p16 status	TP53 status	synthetic lethal nanos1
BJ	wt	wt	no
RPE	wt	wt	no
Calu-1	wt	wt	no
Corl-105	wt	wt	no
SW1573	mut	wt	yes
NCI-H1563	mut	wt	yes
NCI-H1666	mut	wt	yes
T24	wt	mut	no
J82	mut	mut	no
TCCSUP	mut	mut	no
MCF10a	wt	wt	no
MCF7	mut	wt	no
MDA-MB-231	mut	mut	no
FADU	wt	mut	no
JHU029	mut	mut	no
293T	mut	mut	no
HCT-116	mut	wt	yes
Saos2	mut	mut	no



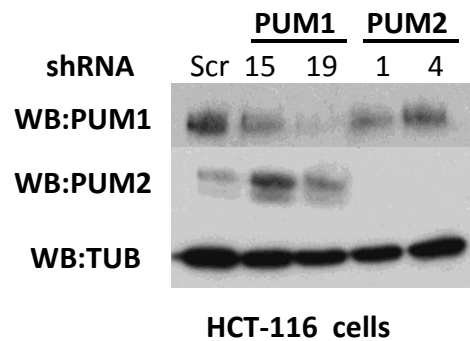
A**B****C**

Miles Supplementary Figure S12: NANOS1 depletion reduces cell number in pRb-deficient cancer cells

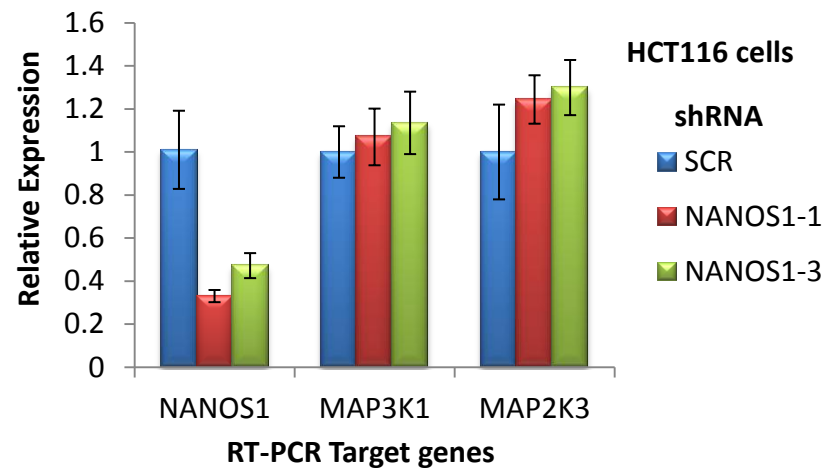


Miles Supplementary Figure S13: Loss of PUM activity stabilizes transcripts down-regulated in Retinoblastoma tumors

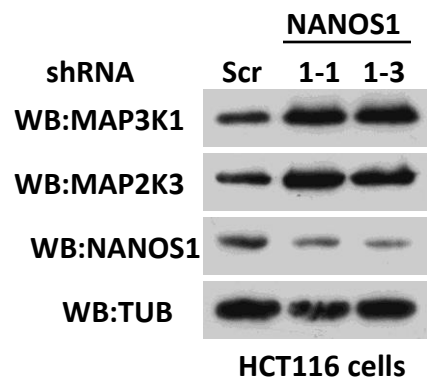
A



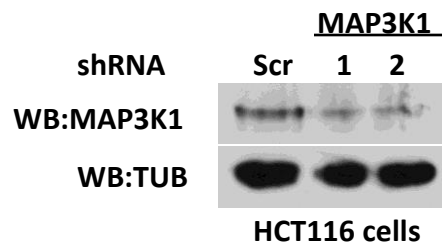
C



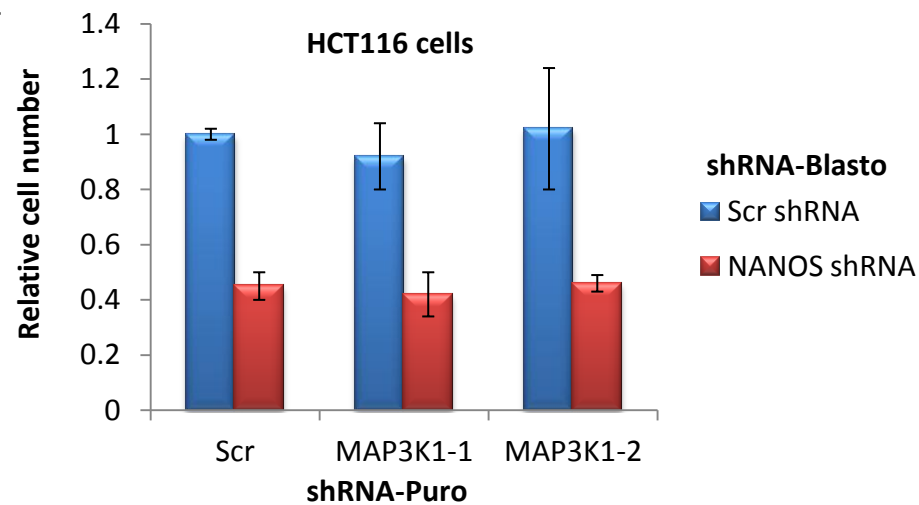
B



D



E



Miles_Supplementary Table S1: Genetic interaction between the Pumilio complex and rbf1

	Nub-Gal4;rbf1-RNAi		<i>rbf1</i> ^{120a}		<i>rbf1</i> ^{120a} /Y;GMR-Gal4/CyO
<i>w</i> ¹¹¹⁸	-	<i>w</i> ¹¹¹⁸	-	Gal4-RNAi	-
Gal4-RNAi	-	<i>pum</i> ¹³	+	pum RNAi	+
GFP-RNAi	-	<i>pum</i> ^{p100c10}	+	nanos RNAi	+
white-RNAi	-	<i>pum</i> ³	-	brat RNAi	+
pum-RNAi (VDRC)	+++	<i>pum</i> ^{msc}	-		
pum-RNAi (TRiP)	+++	<i>nos</i> ^{L7}	+		En-Gal4;e2f2 RNAi
<i>pum</i> ¹³	+	<i>nos</i> ^{J3B6}	+	Gal4-RNAi	-
nanos-RNAi	+++	<i>brat</i> ⁶⁰²⁸	+	pum-RNAi	+
<i>nos</i> ^{L7}	+	<i>brat</i> ¹	+	nanos-RNAi	+
<i>nos</i> ^{J3B6}	+	<i>brat</i> ^{ts1}	+	brat-RNAi	+
brat-RNAi	+++				
<i>brat</i> ^{ts1}	++				
<i>brat</i> ¹	++				

	e2f2 RNAi (03344)	<i>e2f2</i> ^{76Q.1}	<i>dp</i> ^{a3}
Nub-Gal4;Gal4-RNAi	-	-	-
Nub-Gal4;pum-RNAi	+	-	+
Nub-Gal4;nanos-RNAi	+	+	+
Nub-Gal4;brat-RNAi	+	+	+